Analytical theory of the stochastic dynamics of the power stroke in nonprocessive motor proteins

H. J. Woo* and Christopher L. Moss
Department of Chemistry, University of Nevada, Reno, Nevada 89557, USA
(Received 2 August 2005; revised manuscript received 6 September 2005; published 28 November 2005)

Statistical distributions of the structural states of individual molecules of nonprocessive motor complexes such as actomyosins are examined theoretically by considering a two-state stochastic model coupled by chemical reactions along the reaction coordinate representing the internal conformational states of the motor. The use of a conformational reaction coordinate allows for the approximation of taking the rate constants as local in their dependence on the reaction coordinate, and yields a simple analytic solution of the stationary states. The approximation is also tested against numerical solutions with a nonlocal form of rate constants. The theory is well-suited for computational treatments based on atomic structures of protein constituents using free energy molecular dynamics simulations. With empirical sets of free energy functions, stationary distributions of forces exerted by a motor head compare well with known experimental data.

DOI: 10.1103/PhysRevE.72.051924 PACS number(s): 87.16.Nn, 05.40.−a

I. INTRODUCTION

Intensive research efforts have been put recently into understanding the operation of motor proteins with approaches encompassing a wide range of different disciplines. From a fundamental point of view, molecular motor protein complexes such as myosin, kinesin, dynein, or F1-ATPases [1] serve as model systems of how free energy transductions occur in biological systems. Important roles are played both by the stochasticity and irreversibility, each due to the nanometer range of length scales of their protein constituents and the externally controlled nonequilibrium concentrations of adenosine triphosphate (ATP), adenosine diphosphate (ADP), and dissociated inorganic phosphates.

Theoretical considerations based on nonequilibrium statistical mechanics have played important roles in the development of such understandings [2–19]. In particular, the Brownian ratchet model, first described by Feynman as a demonstration of the inevitable reversibility of any macroscopic movements driven by equilibrium fluctuations [20], has provided conceptual guidelines of how free energy transductions could become possible far from equilibrium. A prototypical Brownian ratchet has external controls switching the potential (of mean force, defined below) the Brownian particle feels along a reaction coordinate x (the displacement of a motor head on the linear track) between a flat profile and an asymmetric profile [Fig. 1(a)], resulting in the nonzero average net flux of the particle. Various different versions of the ratchet models have been studied over the past decade using methods of stochastic dynamics [2,3,6,9,13,18].

A largely unresolved question, however, is how the key mechanisms of such theoretical models are implemented in reality within their protein constituents, for which studies have been initiated for F1-ATPase and myosins only recently [4,21,22]. The rapid growth in our structural knowledge of the molecular details of the building blocks comprising the motor complexes [23] is expected to provide us important tests of theoretical models regarding their basic assumptions as well as applicabilities to different specific systems. In this paper, in particular, we argue that attentions to structural details should help resolve some of the issues that have arisen within the studies of motor proteins. One of such issues is

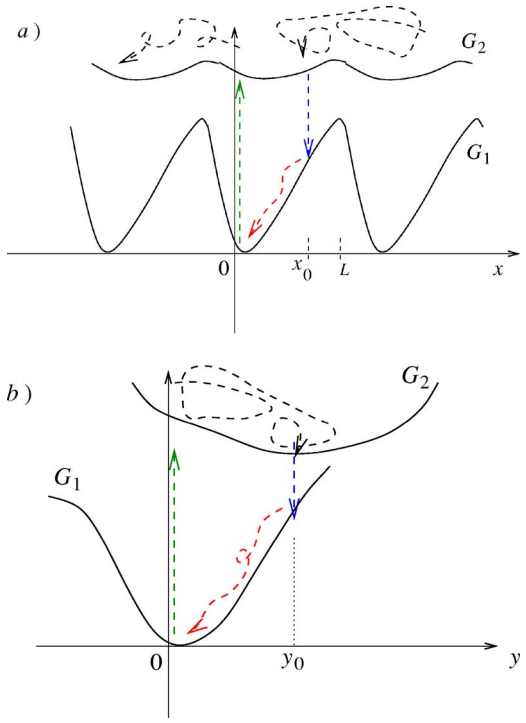

FIG. 1. (Color online) The Brownian ratchet and the power stroke mechanisms as projections of two-dimensional free energy landscapes $G_i(x,y)$ into one-dimensional axes. (a) In the Brownian ratchet models, the stochastic variable x is defined as the linear displacement of the motor protein center-of-mass along the track. (b) The conformational changes of the motor protein occur via the Brownian motion of the conformational reaction coordinate y. See Fig. 3 for the interpretation of the arrows in (a) within the conventional ratchet perspective.

*Author to whom correspondences should be addressed. Email address: woo@chem.unr.edu

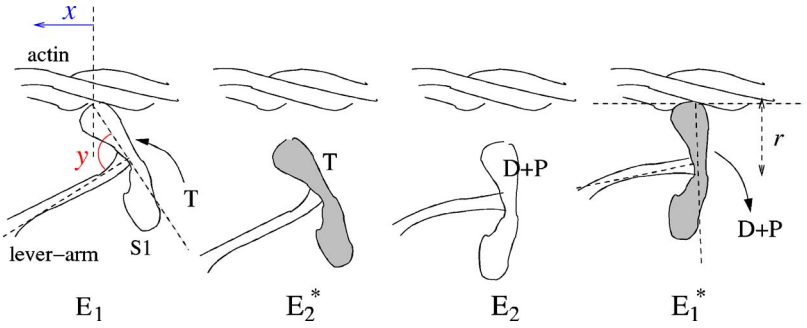

FIG. 2. (Color online) Swinging lever arm mechanism of muscle contraction. The myosin heads in strained states E_1^* and E_2^* are shown as shaded. Binding (unbinding) of S1 to an actin filament facilitates unbinding (binding) of phosphate (P), ATP (T), and ADP (D), and vice versa. The conformational reaction coordinate y is defined here as the lever arm angle, and the distance r between the center of the "hinge" and the actin binding site is also shown.

whether the Brownian ratchet models should be regarded as representing an alternative mechanism [24] superseding the traditional power stroke description exemplified by the swinging lever arm model of muscle contractions [1,25,26]. Qian [15] has pointed out that the issue of the roles played by either the center-of-mass diffusive motion along the track or the concerted intramolecular conformational changes of a motor head is a quantitative question (the two representations in Fig. 1 become projections of a two-dimensional free energy landscape). Wang and Oster [27] have defined the relative weights of the power stroke and ratchet characters of a rotary motor in terms of the fractions of the work done on the load by thermodynamic forces and by Brownian random forces. We expand such a point of view in this paper and show how the quantitative question could be answered by adopting a structure-based theoretical viewpoint, supplemented by methods such as molecular simulations based on known atomic structures.

A second primary aim of the paper is to examine the approach of using the conformational reaction coordinate for the stochastic dynamical model of motor proteins based on the power stroke point of view, by integrating out the displacement axis of the reaction coordinate space. The resulting version of the two-level stochastic model for nonprocessive motor proteins has direct connections to protein structural states, making it particularly useful for future incorporations of molecular simulation results based on atomic structures of proteins. In particular, we use the approximation of taking the reaction coordinate dependence of rate constants as local, which allows us to find a simple analytical solution of nonequilibrium stationary distributions for a general functional form of the potentials of mean force $G_i(y)$. The stationary solution then leads to various measurable quantities of the motor complex on the single-molecule level, some of which are examined here using a quadratic model functional form of G_i with empirical parameters.

The paper is organized as follows. In the next section, the swinging lever arm model of muscle contractions is briefly reviewed with a special emphasis on its relationship to the stochastic dynamics of conformational states. The stochastic dynamical model is motivated from the molecular and structural point of view in Sec. II B through the coarse graining associated with the introduction of two reaction coordinates, the linear displacement and the conformational reaction coordinate. The Brownian ratchet and power stroke perspectives are discussed regarding their inter-relationships in Sec. II C. In Sec. III A, the simple two-level version of the stochastic dynamical model of the conformational reaction coordinate is solved analytically for the nonequilibrium stationary states. The local rate constant approximation used is also tested and justified using Monte Carlo simulations. The stationary solution is used in Sec. III B to examine some of the properties of actomyosin complexes on the single-molecule level, which are compared with experiments. Section IV concludes the paper with a short discussion.

II. MECHANISM OF MOTOR OPERATIONS

A. Muscle contraction

In actomyosin complexes underlying muscle contractions [1,23], myosin heads subfragment 1 (S1) undergo diffusive attachment/detachment cycles onto the actin filaments, while changing its conformational states characterized by distinct orientations of their lever arms (Fig. 2) [25,28]. The biochemical nature of the overall process can be represented by denoting a pair of such states as E_1 and E_2, and writing a simple extension of the Michaelis-Menten mechanism [29,30]

$$\mathrm{E}_1 + \mathrm{T} \underset{k_{-h}}{\overset{k_h}{\rightleftharpoons}} \mathrm{E}_2^* \cdot \mathrm{T} \rightleftharpoons \mathrm{E}_2 \cdot \mathrm{D} \cdot \mathrm{P} \xrightarrow{k_p} \mathrm{E}_1^* + \mathrm{D} + \mathrm{P} \rightleftharpoons \mathrm{E}_1 + \mathrm{D} + \mathrm{P}, \tag{1}$$

where ATP, ADP, and phosphate are represented as T, D, and P, respectively. The enzyme in the two different structural states E_1 and E_2 are distinguished by the presence or absence of the nucleotide substrates in the binding site. The second and fourth steps are the conformational relaxations of the "strained" enzymes E_1^* and E_2^* into their stable states E_1 and E_2. By maintaining a constant supply of the fuel T and preventing accumulations of the products D and P via external matter reservoirs, stationary cyclic processes based on Eq. (1) can be sustained.

Muscle contractions occur by S1 attachment/detachment processes coordinated with the chemical and conformational transitions of scheme (1); E_1 primarily occurs while bound to an actin filament, whereas the myosin head is in solution while in E_2. The cyclic process for actomyosins interpreted in terms of the free energy landscapes in Fig. 1(b) consists of the following four steps.

(a) An ATP binds to an S1 bound to actin, causing its dissociation, which is represented by a vertical jump from the minimum $y=0$ of $G_1(y)$ of E_1 to a strained conformation with free energy $G_2(0)$, or E_2^*.

(b) The motor domain then re-adjusts its conformational state to the new stable state $y=y_0$, which entails the "reprimming" of the lever arm.

(c) With the prepower stroke (transition-state) conformation at $y=y_0$, the ATP binding site catalyzes the hydrolysis of ATP to form ADP and phosphate. The complex binds to the actin again, which leads to the release of phosphate (and ADP).

(d) The resulting conformational relaxation, the *power stroke*, causes a large swinging motion of the lever arm back to its position in the rigor conformation.

It is obvious that the mechanism described above should be regarded as inherently stochastic; conformational changes of a single motor head observed for example in optical tweezer experiments are highly noisy [31–35], adding up to a concerted cyclic process only on average. A number of qualitative observations based on Fig. 1(b) can be made at this point: the prestroke repriming of lever arm on G_2 occurs in solution, and therefore the associated free energy released is completely dissipated. One thus can write for the maximum work derivable from a single power stroke in the reversible limit as

$$W_{\mathrm{rev}} = G_1(y_0) - G_1(0) < \Delta G_h, \tag{2}$$

where $\Delta G_h = G_2(0) - G_1(0)$. The efficiency η then satisfies

$$\eta = \frac{W}{\Delta G_h} < \frac{W_{\mathrm{rev}}}{\Delta G_h} < 1, \tag{3}$$

where W is the (nonreversible) work performed, showing that the efficiency of actomyosin motors is fundamentally limited by the need to "prime" the lever arm while detached, in addition to the intrinsic irreversibility in each step. In contrast, the rotary motor F1-ATPase has three identical subunits each taking turns in the analogous free energy transduction cycles, such that a power-stroke of one subunit becomes the "priming" for another, achieving the efficiency near 100% [36]. For muscle contractions, however, where linear movements on macroscopic scales need to be generated via collective actions of billions of myosin units, the relatively low efficiency near 20% [36] is inevitable, due to the need for repriming the lever arm where the corresponding part of the chemical free energy is completely dissipated.

B. Coarse-graining and reaction coordinates

In equilibrium, the probability distribution of the collection $\mathbf{R}$ of atomic coordinates in the system comprising a motor complex, an actin filament, solvent water molecules, nucleotides, and any ions can be written as

$$P(\mathbf{R}) = \frac{e^{-\beta \hat{V}(\mathbf{R})}}{\int d\mathbf{R} e^{-\beta \hat{V}(\mathbf{R})}}, \tag{4}$$

where $\hat{V}$ is the total potential energy and $1/\beta = k_B T$ is the Boltzmann constant times temperature. A coarse-grained description of the system is made possible by choosing a set of reaction coordinates, which we take as $\{x, y\}$, where x is defined as representing the position of the myosin head center-of-mass along the direction of the actin filament assumed to be fixed, while y is a *conformational* reaction coordinate, dependent on the internal coordinates of the motor complex [15]. Among the possible definitions of y are the lever arm angle shown in Fig. 2, and the relative root-mean-square deviation (RMSD) [37], defined with respect to two known reference structures (e.g., crystal structures) as $\hat{y} = \hat{y}_1 - \hat{y}_2$, where y_j is the RMSD of atomic coordinates within the motor head S1 relative to the reference structure j. The latter choice of y is particularly well-suited for use in free energy calculations using molecular dynamics [37].

The reduced probability distribution of the reaction coordinates is obtained from Eq. (4) as

$$P_i(x,y) = \int_{\mathbf{R}\in i} d\mathbf{R}\, \delta(x-\hat{x})\, \delta(y-\hat{y}) P(\mathbf{R}) = \frac{e^{-\beta G_i(x,y)}}{\sum_i \int dx \int dy e^{-\beta G_i(x,y)}}, \tag{5}$$

where the second line introduces a generalized free energy, or the potential of mean force (PMF) $G_i(x,y)$, defined up to an arbitrary constant as

$$e^{-\beta G_i(x,y)} \propto \int_{\mathbf{R}\in i} d\mathbf{R}\, \delta(x-\hat{x})\, \delta(y-\hat{y}) e^{-\beta \hat{V}(\mathbf{R})}. \tag{6}$$

In Eqs. (5) and (6), we have introduced the set of sub-spaces of the configurational space labeled by $i=1,2$, each corresponding to those with actin-bound S1 without nucleotides, and those with S1 in solution with bound nucleotides. The integrations in Eqs. (5) and (6) are restricted to the respective subspaces.

As is evident from Eq. (6), the introduction of the coarse-grained reaction coordinates entails a drastic reduction in the dimensionality of the configurational space, and the suitability of the particular choice of the reaction coordinate can only be tested by explicit calculations of G_i based on realistic molecular models of the protein. We also note that a very recent study by Fischer *et al.* [38], where a minimum energy path connecting two distinct conformations of myosin head has been identified within the conformational space using computational methods, suggests a near-ideal case for which y could be defined as the progression along such a path.

C. Brownian ratchet vs power stroke

Qualitative considerations of the known structural information of actomyosin complexes as depicted in Fig. 2 naturally lead us to the two different representations of the free energy landscape shown in Fig. 1, with the corresponding PMF defined by

$$e^{-\beta G_i(x)} = \int dy e^{-\beta G_i(x,y)}, \tag{7a}$$

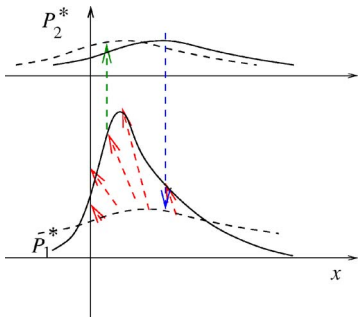

FIG. 3. (Color online) The equivalence of the Brownian ratchet and the power stroke perspectives. P_1^* and P_2^* are the quasiequilibrium distributions of the motor head displacement x under the PMF $G_1(x)$ and $G_2(x)$, respectively [Fig. 1(a)]. After the potential has been switched on to become G_1, the near-uniform distribution (dotted line at the bottom) has to evolve toward P_1^*, generating a net flux equivalent to the power stroke depicted as the downhill drift in Fig. 1(a). Note that the true stationary distributions $P_1(x)$ and $P_2(x)$ will differ from quasiequilibrium ones due to the contributions of transient distributions indicated by arrows.

$$e^{-\beta G_i(y)} = \int dx e^{-\beta G_i(x,y)}. \tag{7b}$$

The asymmetric downhill slope to the left near the binding site x_0 on actin in Fig. 1(a) is a consequence of the relative stability of the near-rigor conformation of E_1 compared to the prestroke E_1^* state, and the fact that the conformational change $E_1^* \rightarrow E_1$ would need to be accompanied by the net movement of the S1 center-of-mass to the right (Fig. 2). In the Brownian ratchet perspective, the net flux is understood as arising from the asymmetric quasiequilibrium distribution established on G_1 in Fig. 1(a), which is subsequently spread over evenly via (almost) free diffusions after the field has been turned off (G_2). If we consider the most probable trajectory of a *single* motor head within the same perspective, however, it would still be represented by the series of arrows depicted in Fig. 1(a), with the "power stroke" of the Brownian ratchet shown as the downhill drifting on G_1 on the actin filament. The power stroke in this case can conversely be interpreted as the *relaxation* towards the establishment of the asymmetric distribution of motor head position on G_1 within the former perspective, which is unavoidable in order for any subsequent ratcheting to occur (Fig. 3).

Within the unified point of view based on the general PMF $G_i(x,y)$ and its one-dimensional projections, therefore, the distinction between the two seemingly different perspectives becomes a quantitative one [15]. The difference in particular centers on the extent to which the stochastic dynamics of the motor head reaction coordinate, largely on $G_2(y)$, is affected by the thermal diffusion or concerted relaxations toward the minimum in free energy. The question needs to be addressed based on considerations of molecular structures, for example, by calculating the diffusion coefficients of the motor head on the PMF, which can be obtained using molecular simulation techniques [39]. In this paper, we adopt the version of description using the free energy landscape of the conformational reaction coordinate y represented by Fig. 1(b). The choice is appropriate for nonprocessive motor protein systems such as actomyosins, where a typical motor complex is expected to undergo more concerted movements on average in its conformational space than in its positional displacement.

III. STOCHASTIC DYNAMICS

The coarse graining of the level of description from the full phase space variables $\mathbf{R}$ to the low-dimensional reaction coordinates naturally renders the relevant dynamics to be stochastic. The simplest such dynamics in the absence of coupling between G_1 and G_2 can be described by the Langevin equation

$$0 = F_{\text{ex}} - G_i'(y) - \gamma_i \dot{y} + \zeta_i(t), \tag{8}$$

where the overdamping has been assumed ($\ddot{y} \simeq 0$), F_{ex} is the external load, $G_i'(y) \equiv dG_i/dy$, γ_i is the friction coefficient, and the random forces $\zeta_i(t)$ have zero means and are uncorrelated:

$$\langle \zeta_i(t) \rangle = 0,$$

$$\langle \zeta_i(t) \zeta_i(t') \rangle = 2\gamma_i k_B T \delta(t-t'). \tag{9}$$

Equation (8) precludes the reactions that couple states in different subgroups i, which can be incorporated more easily in the equivalent Fokker-Planck description as follows [6,12]:

$$\frac{\partial P_1}{\partial t} = -\frac{\partial J_1}{\partial y} - k_h(y) c P_1 + k_{-h}(y) P_2 + k_p(y) P_2,$$

$$\frac{\partial P_2}{\partial t} = -\frac{\partial J_2}{\partial y} + k_h(y) c P_1 - k_{-h}(y) P_2 - k_p(y) P_2, \tag{10}$$

where J_i is the flux on the free energy curve i given phenomenologically by the linear constitutive relation

$$J_i = \bar{v}_i P_i - D_i \frac{\partial P_i}{\partial y}. \tag{11}$$

In Eq. (11), D_i is the diffusion coefficient, and the deterministic velocity $\bar{v}_i$ in the simplified Smoluchowsky description is obtained from the balance of the external load, the thermodynamic force $-G_i'$, and the frictional drag $-\gamma_i \bar{v}_i$:

$$F_{\text{ex}} - G_i' - \gamma_i \bar{v}_i = 0 \tag{12}$$

or

$$\bar{v}_i = \frac{F_{\text{ex}} - G_i'}{\gamma_i}. \tag{13}$$

The rate constants k_h, k_{-h}, and k_p are those for the ATP binding (actin unbinding), the reverse reaction of ATP unbinding (actin binding), and the prestroke dissociation of phosphate (actin binding), respectively [Fig. 1(b)]. We ignore the rate of reverse reaction corresponding to k_p, known to be negligible in reality [40]. The y dependence of the rate constants reflects the expectation that the catalyzed rates of each reactions would depend strongly on the protein conformation.

The concentration of ATP is denoted as c, assumed to be maintained as constant throughout the system by external controls.

A. Local rate constant approximation

For the reaction coordinate dependence of the rate constants, we use the local rate constant approximation

$$k_h(y) = k_h\delta(y),$$

$$k_{-h}(y) = k_{-h}\delta(y),$$

$$k_p(y) = k_p\delta(y - y_0), \tag{14}$$

justified by the fact that the magnitude of the conformational change [y_0 in Fig. 1(b)] between the two minima is much larger (of the order of 10 Å) than the range of fluctuations around each structural state within which the reaction catalysis remains effective. The use of delta functions for the rate constants' dependence on the center-of-mass displacement x along the filament has previously been considered by Jülicher *et al.* [13] in the context of processive motor proteins. Bagdassarian and Astumian [41] have also used delta function rates in their treatment of conformational fluctuations of membrane transporters. However, only the simplest piecewise linear potential models have been considered in both studies.

In regions where $y \neq 0$ and $y \neq y_0$, the stationary solution $\bar{P}_i(y)$ to Eqs. (10) for which $\partial P_i/\partial t = 0$ satisfies $J_i = c_i = \text{const.}$, or from Eq. (11),

$$\frac{\partial \bar{P}_i}{\partial y} = -\frac{c_i}{D_i} + \beta_i(F_{\text{ex}} - G_i')\bar{P}_i, \tag{15}$$

where $\beta_i \equiv 1/D_i\gamma_i$. A general solution to Eq. (15) can be written as

$$\bar{P}_i^{(n)} = A_i^{(n)} e^{\beta_i[F_{\text{ex}}y - G_i(y)]} + B_i^{(n)} e^{\beta_i[F_{\text{ex}}y - G_i(y)]} \int_0^y dz e^{\beta[G_i(z) - F_{\text{ex}}z]}, \tag{16}$$

where $A_i^{(n)}$ and $B_i^{(n)} = -c_i/D_i$ are the coefficients to be determined by the boundary conditions for $\bar{P}_i^{(n)}$, and the superscripts with $n = 1, 2, 3$ distinguish three different regions $y < 0$, $0 < y < y_0$, and $y > y_0$, respectively. Since

$$\lim_{y \to \pm\infty} [G_i(y) - F_{\text{ex}}y] = \infty \tag{17}$$

for constant F_{ex}, $B_i^{(1)} = B_i^{(3)} = 0$. In particular, when the rate constants vanish for all y, $\bar{P}_i$ has to reduce to the equilibrium distribution

$$\bar{P}_i \propto e^{[F_{\text{ex}}y - G_i(y)]/k_BT} \tag{18}$$

from which follows the Einstein relation $\beta_i = 1/k_BT = \beta$ or

$$D_i = \frac{k_BT}{\gamma_i}. \tag{19}$$

For the intermediate region $0 < y < y_0$, $B_i^{(2)} \neq 0$ in general. Imposing the boundary conditions at $y = 0$ and $y = y_0$, the following general solution can be obtained (Appendix A):

$$\frac{\bar{P}_1(y)}{N} = \begin{cases} e^{\beta[F_{\text{ex}}y - G_1(y)]} & (y < 0), \\ e^{\beta[F_{\text{ex}}y - G_1(y)]}\left[1 + \dfrac{ck_hk_pg_1f_2D_2}{D_1Q}\displaystyle\int_0^y dz e^{\beta[G_1(z) - F_{\text{ex}}z]}\right] & (0 < y < y_0), \\ \left(1 + \dfrac{c\Sigma_1k_hk_pg_1f_2D_2}{D_1Q}\right)e^{\beta[F_{\text{ex}}y - G_1(y)]} & (y_0 < y), \end{cases} \tag{20a}$$

$$\frac{\bar{P}_2(y)}{N} = \begin{cases} \dfrac{ck_hg_1(D_2 + k_pf_2\Sigma_2)}{Q}e^{\beta[F_{\text{ex}}y - G_2(y)]} & (y < 0), \\ \dfrac{ck_hg_1}{Q}e^{\beta[F_{\text{ex}}y - G_2(y)]}\left[D_2 + k_pf_2\Sigma_2 - k_pf_2\displaystyle\int_0^y dz e^{\beta[G_2(z) - F_{\text{ex}}z]}\right] & (0 < y < y_0), \\ \dfrac{ck_hg_1D_2}{Q}e^{\beta[F_{\text{ex}}y - G_2(y)]} & (y_0 < y), \end{cases} \tag{20b}$$

where N is the normalization constant determined by $\int dy[\bar{P}_1(y) + \bar{P}_2(y)] = 1$, and

$$\Sigma_i = \int_0^{y_0} dz e^{\beta[G_i(z) - F_{\text{ex}}z]},$$

$$g_i = e^{-\beta G_i(0)},$$

$$f_2 = e^{\beta[F_{\text{ex}}y_0 - G_2(y_0)]},$$

$$Q = (k_{-h}g_2 + k_pf_2)D_2 + k_{-h}k_pf_2g_2\Sigma_2. \tag{21}$$

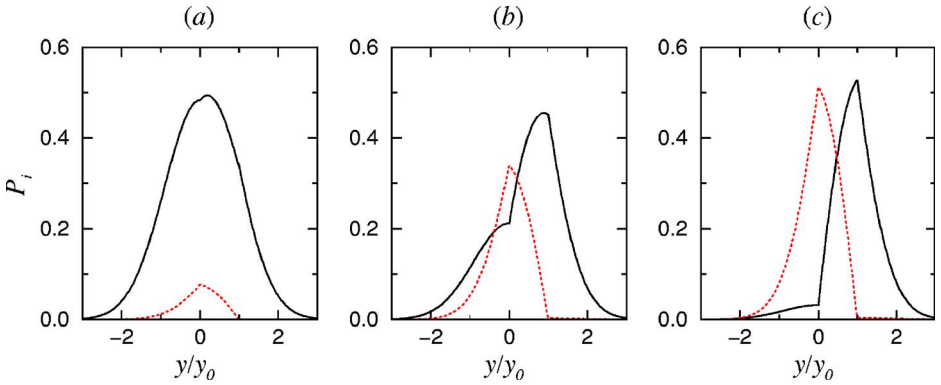

FIG. 4. (Color online) The stationary population $\bar{P}_1(y)$ (solid lines) and $\bar{P}_2(y)$ (dotted lines) at various different ATP concentrations: (a) $c=0.01$, (b) $c=0.1$, (c) $c=1$ μM. Other parameter values are $\beta\kappa_1=\beta\kappa_2=2$, $y_0=\pi/4$, $D_1=D_2=0.2$ s^{-1}, and $F_{ex}=0$.

As a simplest model potential based on Fig. 1(b), we take

$$G_1(y)=\frac{1}{2}\kappa_1 y^2,$$

$$G_2(y)=\frac{1}{2}\kappa_2(y-y_0)^2+\Delta G, \tag{22}$$

for which Fig. 4 shows that the pair of stationary distributions show increasingly sharp deviations from the equilibrium Gaussian shape as c increases from zero, where the rate constant values measured in a kinetic experiment [40] were used; $k_h=6\times10^6$ M^{-1} s^{-1}, $k_{-h}=0$, and $k_p=45$ s^{-1}. The deviations in the region $0<y<y_0$ of the stationary distribution $\bar{P}_1(y)$ and $\bar{P}_2(y)$ (Fig. 4), and the cusps at $y=0$ and $y=y_0$ in particular, are due to the one-sided cyclic flux shown in Fig. 1(b).

We note a number of features from the stationary solution (20); for $c=0$ or $k_h=0$, it reduces to the equilibrium distribution of E_1, Eq. (18), whereas $\bar{P}_2=0$ since the rate at $y=y_0$ is one-sided toward G_1. When $y_0=0$, it is verified that the detailed balance

$$ck_h\bar{P}_1=(k_p+k_{-h})\bar{P}_2 \tag{23}$$

is satisfied at $y=0$. For $y_0\neq0$ in general, the detailed balance is broken both at $y=0$ and $y=y_0$. It should also be noted that in our simplified treatment of chemical reactions where the phosphate release rate at $y=y_0$ is one-sided and we have chosen $k_{-h}=0$, the more general detailed balance condition often invoked in theoretical models, $k_{1\leftarrow2}(y)/k_{2\leftarrow1}(y)=\exp\{-\beta[G_1(y)-G_2(y)]\}$, is not satisfied. An establishment of equilibrium between nonvanishing populations of $G_1(y)$ and $G_2(y)$ is therefore precluded. Although generalizations to remove such a restriction should be straightforward, the fact that the biochemical rates of proteins are expected to be optimized for the predominant cyclic fluxes in Fig. 1(b) makes such an equilibrium state physically rather irrelevant.

The effects of nonlocal dependence of rate constants on reaction coordinate have also been examined using the following generalized form of Eqs. (14):

$$k_h(y)=\frac{k_h}{(2\pi)^{1/2}\sigma_h}e^{-y^2/2\sigma_h^2},$$

$$k_{-h}(y)=\frac{k_{-h}}{(2\pi)^{1/2}\sigma_{-h}}e^{-y^2/2\sigma_{-h}^2},$$

$$k_p(y)=\frac{k_p}{(2\pi)^{1/2}\sigma_p}e^{-(y-y_0)^2/2\sigma_p^2}, \tag{24}$$

where σ_h, σ_{-h}, and σ_p represent the widths of the Gaussian distribution of rates around their centers (Appendix B). Figure 5 shows the typical behavior of stationary distributions as functions of the nonlocal character of the rate constants represented by the width parameter $\sigma_h=\sigma_p=\sigma_{-h}\equiv\sigma$. As σ increases from zero, the strong asymmetry of $\bar{P}_i$ becomes quickly rounded off, and for $\sigma\gtrsim0.3$ in radians, the stationary states appear near equilibrium for $c=0.1$ μM. The mean value of y on the level 1,

$$\langle y\rangle_1=\frac{\int dyyP_1(y)}{\int dyP_1(y)} \tag{25}$$

is a scalar measure of the nonequilibrium character of stationary states, and as shown in Fig. 6, analogously displays a rapid quenching of the asymmetry as σ increases.

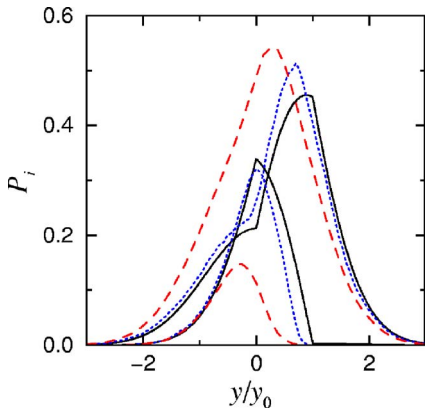

FIG. 5. (Color online) Stationary distributions of P_1 and P_2 with different width of rate constants σ in Eqs. (24). The solid, dotted, and dashed lines are for $\sigma=0$ from Eqs. (20), and the Monte Carlo results for $\sigma=0.1$ and 0.3, respectively. Parameter values are the same as in Fig. 4 with $c=0.1$ μM and $k_{-h}=0$.

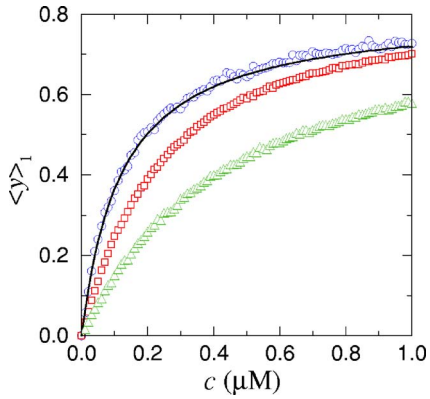

FIG. 6. (Color online) The mean value $\langle y \rangle_1$ averaged over the distribution P_1 as a function of c with different values of σ. The solid line is for $\sigma=0$ from Eqs. (20a), and the circles, squares, and triangles are the Monte Carlo data for 0.01, 0.2, and 0.3, respectively. Parameter values are the same as in Fig. 4.

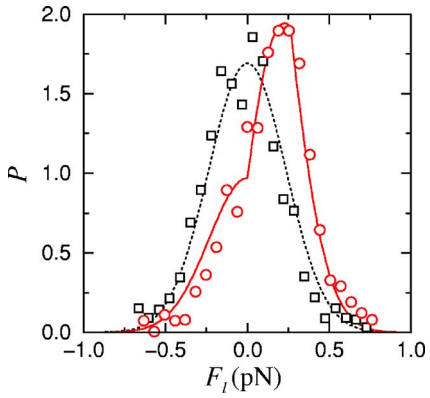

FIG. 7. (Color online) Distribution $P(F_l)$ of forces exerted by a myosin head to the actin filament while bound. The dotted and solid lines are from Eqs. (20a) and (26) with $c=0$ and 0.1 μM, respectively. The rectangles and circles are the experimental data in the given conditions from Ref. [33]. Parameter values are the same as in Fig. 4 except $D_1=D_2=0.22$ s^{-1}.

The strongly nonuniform reaction coordinate dependence of rate constants is thus essential for the production of nonequilibrium stationary states, which sustains the asymmetric cyclic flux shown in Fig. 1 by spatial segregations of different reactions in conformational spaces. Direct measurements or computations of such reaction coordinate dependences of rate constants are difficult in practice, and the local rate constant approximation (14) can serve as physically reasonable and quantitatively reliable assumption which allows for a drastic simplification of the analysis of stochastic dynamical models.

B. Measurable properties in stationary states

Statistical distribution of forces exerted by a single molecule of S1 has been measured in optical tweezer experiments [33]. Taking the reaction coordinate y as the angle of the lever arm, the longitudinal force F_l exerted on the actin filament is related to the thermodynamic force (torque) by $-rF_l=-G_1'(y)=-\kappa_1 y$, where r is the distance between the center of lever arm rotation and the actin binding site (Fig. 2). The distribution of forces exerted while bound is therefore given by

$$P(F_l) \propto \int dy\, \delta(rF_l + \kappa_1 y) P_1(y) \propto P_1(-rF_l/\kappa_1). \quad (26)$$

Figure 7 shows a comparison of the theoretical result (20) and the experimental data from the optical tweezer experiment from Ref. [33] using Eq. (26) and the estimated values of the structural parameters $y_0=\pi/4$ and $r=6$ nm based on the crystallographic structure of myosin [42]. In the absence of ATP ($c=0$), the force distribution is symmetric, and the width of its distribution allows for the determination of the harmonic free energy parameter $\beta\kappa_1=2$, which includes the stiffness contribution arising from the optical trap specific to the experiment. With $c=0.1$ μM, a nonvanishing average of the forces develops, which would translate into the sliding motion of the filament. The use of adjustible parameters in fitting Eq. (20a) to the experimental data in Fig. 7 limits its implications under the current treatment. Using results of first-principle calculations of $G_i(y)$ based on molecular simulations could potentially provide unambiguous tests of the theoretical assumptions.

An example of the mean quantities derivable from P_i is the average force $\langle F_l \rangle$, which will be proportional to $\langle y \rangle_1$ shown in Fig. 6 on a single-molecule level. The qualitative behavior shown in Fig. 6 agrees well with the typical results of *in vitro* motility assays measuring the stationary sliding velocity of the filaments. The proportionality constant of the mean force to the sliding velocity would be equal to the effective friction coefficient of the motion in the x direction, and would most likely reflect strong effects of intermolecular interaction and coordinations beyond the level of description in the current paper.

IV. CONCLUSION

The use of a conformational reaction coordinate offers a useful platform to describe the nonequilibrium stochastic dynamics of nonprocessive motor proteins such as actomyosins, via the PMF $G_i(y)$ that has direct connections to structural aspects of the protein constituents. In particular, explicit calculations of the energy landscapes as well as the dynamical properties such as the diffusion coefficients (via the Green-Kubo relation) using techniques of molecular simulations [43–47] would allow promising directions of bridging simple models of statistical physics, atomic structures from crystallographic studies, and single-molecule experiments.

The local rate constant approximation, justified by the essential nature of the strongly nonuniform conformational dependence of rate constants in sustaining nonequilibrium conditions, allows for a simple and general analytical form of stationary solutions. The model results represented by Eqs. (20), or its more refined variants, valid for arbitrary functions $G_i(y)$, could play useful roles in many other similar formulations for different systems.

ACKNOWLEDGMENTS

We thank Kent Ervin, Sean Casey, and David Leitner for many insightful comments and suggestions.

APPENDIX A: STATIONARY SOLUTION

The boundary conditions at $y=0$ and $y=y_0$ include the continuity of $\bar{P}_i$:

$$\bar{P}_1(0^+) = \bar{P}_1(0^-),$$

$$\bar{P}_2(0^+) = \bar{P}_1(0^-),$$

$$\bar{P}_1(y_0^+) = \bar{P}_1(y_0^-),$$

$$\bar{P}_2(y_0^+) = \bar{P}_1(y_0^-). \tag{A1}$$

In contrast, the functions $\bar{P}_i$ are not differentiable at the two boundary points. We integrate both sides of Eqs. (10) over an immediate neighborhood of the singular points to determine the boundary conditions for the first derivatives, which yields

$$\bar{P}_1'(0^+) - \bar{P}_1'(0^-) = \frac{k_h c}{D_1}\bar{P}_1(0) - \frac{k_{-h}}{D_1}\bar{P}_2(0),$$

$$\bar{P}_2'(0^+) - \bar{P}_2'(0^-) = -\frac{k_h c}{D_2}\bar{P}_1(0) + \frac{k_{-h}}{D_2}\bar{P}_2(0),$$

$$\bar{P}_1'(y_0^+) - \bar{P}_1'(y_0^-) = -\frac{k_p}{D_1}\bar{P}_2(y_0),$$

$$\bar{P}_2'(y_0^+) - \bar{P}_2'(y_0^-) = \frac{k_p}{D_2}\bar{P}_2(y_0), \tag{A2}$$

where $\bar{P}_i'(y) \equiv d\bar{P}_i/dy$. Using Eq. (16) for Eq. (A2), the determination of the unknown coefficients $\{A_i^{(n)}, B_i^{(n)}\}$ is facilitated by expressing the boundary conditions as matrix equations

$$\mathbf{C}^{(n)} = \begin{bmatrix} A_1^{(n)} \\ B_1^{(n)} \\ A_2^{(n)} \\ B_2^{(n)} \end{bmatrix} \tag{A3}$$

and

$$\mathbf{C}^{(3)} = \mathsf{M}_{32}\mathbf{C}^{(2)} = \mathsf{M}_{32}\mathsf{M}_{21}\mathbf{C}^{(1)} \equiv \mathsf{M}_{31}\mathbf{C}^{(1)}. \tag{A4}$$

From the boundary conditions (A1) and (A2), the matrices are given by

$$\mathsf{M}_{21} = \begin{bmatrix} 1 & 0 & 0 & 0 \\ ck_h g_1/D_1 & 1 & -k_{-h}g_2/D_1 & 0 \\ 0 & 0 & 1 & 0 \\ -ck_h g_1/D_2 & 0 & k_{-h}g_2/D_2 & 1 \end{bmatrix},$$

$$\mathsf{M}_{32} = \begin{bmatrix} 1 & 0 & \Sigma_1 k_p f_2/D_1 & \Sigma_1\Sigma_2 k_p f_2/D_1 \\ 0 & 1 & -k_p f_2/D_1 & -k_p f_2 \Sigma_2/D_1 \\ 0 & 0 & 1-\Sigma_2 k_p f_2/D_2 & -\Sigma_2^2 k_p f_2/D_2 \\ 0 & 0 & k_p f_2/D_2 & \Sigma_2 k_p f_2/D_2 + 1 \end{bmatrix}, \tag{A5}$$

where Σ_i, g_i, and f_2 are given by Eqs. (21), and

$$\mathsf{M}_{31} = \begin{bmatrix} 1-\dfrac{\Sigma_1\Sigma_2 k_p f_2 ck_h g_1}{D_1 D_2} & 0 & \dfrac{\Sigma_1 k_p f_2}{D_1} + \dfrac{\Sigma_1\Sigma_2 k_p f_2 k_{-h} g_2}{D_1 D_2} & \dfrac{\Sigma_1\Sigma_2 k_p f_2}{D_1} \\ \dfrac{ck_h g_1}{D_1} + \dfrac{k_p f_2 \Sigma_2 ck_h g_1}{D_1 D_2} & 1 & -\dfrac{k_{-h}g_2}{D_1} - \dfrac{k_p f_2}{D_1} - \dfrac{k_p k_{-h} f_2 \Sigma_2 g_2}{D_1 D_2} & -\dfrac{k_p f_2 \Sigma_2}{D_1} \\ \dfrac{ck_h g_1 \Sigma_2^2 k_p f_2}{D_2^2} & 0 & 1-\dfrac{\Sigma_2 k_p f_2}{D_2} - \dfrac{\Sigma_2^2 k_p f_2 k_{-h} g_2}{D_2^2} & -\dfrac{\Sigma_2^2 k_p f_2}{D_2} \\ -\dfrac{ck_h g_1}{D_2}\left(\dfrac{\Sigma_2 k_p f_2}{D_2}+1\right) & 0 & \dfrac{k_p f_2}{D_2} + \dfrac{k_{-h}g_2}{D_2}\left(\dfrac{\Sigma_2 k_p f_2}{D_2}+1\right) & \dfrac{\Sigma_2 k_p f_2}{D_2}+1 \end{bmatrix}. \tag{A6}$$

Imposing the boundary conditions at $y=\pm\infty$, $B_i^{(1)}=B_i^{(3)}=0$ using Eq. (A6), the following relation can be obtained:

$$A_2^{(1)} = \frac{ck_h g_1}{Q}(D_2 + k_p f_2 \Sigma_2) A_1^{(1)}, \tag{A7}$$

where Q is defined in Eqs. (21). It should be noted that the two conditions $B_1^{(3)}=0$ and $B_2^{(3)}=0$ in fact both lead to Eq. (A7), which is due to the overall conservation law of the total probability

$$\frac{\partial}{\partial t}(P_1 + P_2) = -\frac{\partial}{\partial y}(J_1 + J_2) \tag{A8}$$

from Eqs. (10). Using Eqs. (A4), (A6), and (A7), the remaining nonvanishing coefficients can all be expressed in terms of $A_1^{(1)}$:

$$A_1^{(2)} = A_1^{(1)},$$

$$B_1^{(2)} = \frac{ck_h g_1 k_p f_2 D_2}{D_1 Q} A_1^{(1)},$$

$$A_1^{(3)} = 1 + \frac{\Sigma_1 k_p f_2 g_1 c k_h D_2}{D_1 Q} A_1^{(1)},$$

$$A_2^{(1)} = A_2^{(2)} = \frac{ck_h g_1}{Q}(D_2 + k_p f_2 \Sigma_2) A_1^{(1)},$$

$$B_2^{(2)} = -\frac{ck_h k_p f_2 g_1}{Q} A_1^{(1)},$$

$$A_2^{(3)} = \frac{ck_h g_1 D_2}{Q} A_1^{(1)}. \tag{A9}$$

The normalization condition fixes the last coefficient $A_1^{(1)}$, and the solution (20) is obtained.

APPENDIX B: MONTE CARLO SIMULATIONS

Direct Monte Carlo simulations were performed to solve the stochastic model defined by the Fokker-Planck equations (10) with the nonlocal form of the rate constants (24). We can write the equivalent Langevin representation in discretized form as follows:

$$y_{n+1} = y_n + \dot{y}_n \Delta t,$$

$$\dot{y}_n = \sum_{i=1,2} \delta_{i l_n} [- D_i \beta G_i'(y_n) + f_{in}], \tag{B1}$$

where y_n is the value of y at time $t = t_0 + n\Delta t$ ($n = 0, 1, \ldots$) and $\delta_{i l_n}$ is the Kronecker delta, in which $l_n = 1, 2$ is a dynamical binary variable representing which of the two levels the system is residing at a time $t = t_n$, evolving with the transition probabilities

$$P_{2 \leftarrow 1} = c k_h(y_n) \delta_{1 l_n},$$

$$P_{1 \leftarrow 2} = [k_{-h}(y_n) + k_p(y_n)] \delta_{2 l_n}. \tag{B2}$$

The random forces f_{in} on the level i at time t_n are taken from Gaussian distributions such that

$$\langle f_{in} \rangle = 0,$$

$$\langle f_{in} f_{jm} \rangle = \frac{2D_i}{\Delta t} \delta_{ij} \delta_{nm}. \tag{B3}$$

At each time step, the displacement and the jump moves, each given by Eqs. (B1) and (B2) were attempted with equal probabilities, and the stationary distributions of $P_1(y)$ and $P_2(y)$ were constructed by collecting histograms over the time domain. The time step and the number of steps used were $\Delta t = 10^{-2}$ sec and $N = 3 \times 10^7$ for most cases, except for very small width of rate constants, for which we used $\Delta t = 10^{-4}$ s and $N = 10^9$.

[1] R. D. Vale and R. A. Milligan, Science **288**, 88 (2000).
[2] R. D. Astumian and M. Bier, Phys. Rev. Lett. **72**, 1766 (1994).
[3] C. Bustamante, D. Keller, and G. Oster, Acc. Chem. Res. **34**, 412 (2001).
[4] H. Y. Wang and G. Oster, Nature (London) **396**, 279 (1998).
[5] S. Leibler and D. A. Huse, J. Cell Biol. **121**, 1357 (1993).
[6] P. Reimann, Phys. Rep. **361**, 57 (2002).
[7] M. E. Fisher and A. B. Kolomeisky, Proc. Natl. Acad. Sci. U.S.A. **96**, 6597 (1999).
[8] M. Bier, Phys. Rev. Lett. **91**, 148104 (2003).
[9] A. Parmeggiani, F. Jülicher, A. Ajdari, and J. Prost, Phys. Rev. E **60**, 2127 (1999).
[10] J. F. Chauwin, A. Ajdari, and J. Prost, Europhys. Lett. **27**, 421 (1994).
[11] J. F. Chauwin, A. Ajdari, and J. Prost, Europhys. Lett. **32**, 373 (1995).
[12] J. Prost, J. F. Chauwin, L. Peliti, and A. Ajdari, Phys. Rev. Lett. **72**, 2652 (1994).
[13] F. Jülicher, A. Ajdari, and J. Prost, Rev. Mod. Phys. **69**, 1269 (1997).
[14] H. Qian, Biophys. Chem. **67**, 263 (1997).
[15] H. Qian, Phys. Rev. Lett. **81**, 3063 (1998).
[16] H. Qian, Phys. Rev. E **69**, 012901 (2004).
[17] R. D. Astumian and I. Derenyi, Biophys. J. **77**, 993 (1999).
[18] R. D. Astumian, Science **276**, 917 (1997).
[19] T. A. Duke, Proc. Natl. Acad. Sci. U.S.A. **96**, 2770 (1999).
[20] R. P. Feynman, R. B. Leighton, and M. Sands, *The Feynman Lectures on Physics* (Addison-Wesley, Reading, MA, 1963), Vol. I.
[21] G. Lan and S. X. Sun, Biophys. J. **88**, 4107 (2005).
[22] G. Lan and S. X. Sun, Biophys. J. **88**, 999 (2005).
[23] M. A. Geeves and K. C. Holmes, Annu. Rev. Biochem. **68**, 687 (1999).
[24] W. Herzog and R. Ait-Haddou, J. Electromyogr. Kinesiol. **12**, 425 (2002).
[25] R. W. Lymn and E. W. Taylor, Biochemistry **10**, 4617 (1971).
[26] R. Cooke, J. Gen. Physiol. **123**, 643 (2004).
[27] H. Y. Wang and G. Oster, Appl. Phys. A: Mater. Sci. Process. **75**, 315 (2002).
[28] H. E. Huxley, Science **164**, 1356 (1969).
[29] E. Eisenberg and T. L. Hill, Science **227**, 999 (1985).
[30] D. A. Smith and M. A. Geeves, Biophys. J. **69**, 524 (1995).
[31] J. T. Finer, R. M. Simmons, and J. A. Spudich, Nature (London) **368**, 113 (1994).
[32] K. Kitamura, M. Tokunaga, A. H. Iwane, and T. Yanagida, Nature (London) **397**, 129 (1999).
[33] A. Ishijima, H. Kojima, T. Funatsu, M. Tokunaga, H. Higuchi, H. Tanaka, and T. Yanagida, Cell **92**, 161 (1998).
[34] H. Noji, R. Yasuda, M. Yoshida, and K. Kinosita, Nature (London) **386**, 299 (1997).

[35] R. Yasuda, H. Noji, M. Yoshida, K. Kinosita, and H. Itoh, Nature (London) **410**, 898 (2001).
[36] K. Kinosita, Jr., R. Yasuda, H. Noji, S. Ishiwata, and M. Yoshida, Cell **93**, 21 (1998).
[37] N. K. Banavali and B. Roux, J. Am. Chem. Soc. **127**, 6866 (2005).
[38] S. Fischer, B. Windshügel, D. Horak, K. C. Holmes, and J. C. Smith, Proc. Natl. Acad. Sci. U.S.A. **102**, 6873 (2005).
[39] H. J. Woo (unpublished).
[40] M. Brune, J. L. Hunter, J. E. T. Corrie, and M. R. Webb, Biochemistry **33**, 8262 (1994).
[41] C. K. Bagdassarian and R. D. Astumian, in *Thermodynamics in Biology*, edited by E. di Cera (Oxford, New York, 2000), pp. 203–225.
[42] A. Houdusse, V. N. Kalbokis, D. Himmel, A. G. Szent-Gyorgyi, and C. Cohen, Cell **97**, 459 (1999).
[43] P. Kollman, Chem. Rev. (Washington, D.C.) **93**, 2395 (1993).
[44] T. Simonson, G. Archontis, and M. Karplus, Acc. Chem. Res. **35**, 430 (2002).
[45] G. M. Torrie and J. P. Valleau, J. Comput. Phys. **23**, 187 (1977).
[46] S. Kumar, D. Bouzida, R. H. Swendsen, P. A. Kollman, and J. M. Rosenberg, J. Comput. Chem. **13**, 1011 (1992).
[47] S. Bernèche and B. Roux, Nature (London) **414**, 73 (2001).